

CASE REPORT

A novel *de novo* missense mutation in *EFTUD2* identified by whole-exome sequencing in mandibulofacial dysostosis with microcephaly

Mei Yang^{1,2}  | Yanyan Liu^{1,2}  | Ziyuan Lin^{2,3,4} | Huaqin Sun^{2,3,4}  | Ting Hu^{1,2} 

¹Department of Medical Genetics, West China Second University Hospital, Sichuan University, Chengdu, Sichuan, China

²Key Laboratory of Birth Defects and Related Diseases of Women and Children (Sichuan University), Ministry of Education, Chengdu, China

³SCU-CUHK Joint Laboratory for Reproductive Medicine, West China Second University Hospital, Sichuan University, Chengdu, Sichuan, China

⁴Department of Pediatrics, West China Second University Hospital, Sichuan University, Chengdu, Sichuan, China

Correspondence

Huaqin Sun and Ting Hu, No. 20, Section 3, Renminnan Road, Chengdu, Sichuan, 610041, China.

Emails: sunhuaqin@scu.edu.cn (H. S.); huting4123@163.com (T. H.)

Funding information

National Key Research and Development Program of China, Grant/Award Number: 2021YFC1005304

Abstract

Background: Mandibulofacial dysostosis with microcephaly (MFDM) is a rare multiple malformation syndrome characterized by malar and mandibular hypoplasia and congenital- or postnatal-onset microcephaly induced by haploinsufficiency of (elongation factor Tu GTP-binding domain-containing 2) *EFTUD2*.

Methods: We report the case of a 16-month-old boy with MFDM symptoms, including malar and mandibular hypoplasia, microcephaly, micrognathia, midline cleft palate, microtia, auditory canal atresia, severe sensorineural hearing loss, and developmental delay. Whole-exome sequencing (WES) analysis of the patient's family was performed to identify the genetic etiology responsible for this phenotype.

Results: We identified a novel *de novo* missense mutation (c.671G>T, p.Gly224Val) in the *EFTUD2*. According to the American College of Medical Genetics and Genomics (ACMG) 2015 guidelines, the c.671G>T mutation was classified as likely pathogenic (PS2, PM1, PM2, and PP3). Based on our findings, prenatal diagnosis was performed on the second baby of the proband's parents to exclude the mutation and it was confirmed that the baby did not have the MFDM phenotype after 14 months of follow-up. Furthermore, the zebrafish model confirmed that the *EFTUD2* c.671G>T mutation caused a loss of gene function in *EFTUD2*, and the pathogenicity of the *EFTUD2* c.671G>T mutation was classified as pathogenic (PS2, PS3, PM1, and PM2).

Conclusion: Our results indicate that WES is a useful tool for identifying potentially pathogenic mutations, particularly in rare disorders, and is advantageous for genetic counseling and subsequent prenatal diagnosis. Moreover, the importance of functional assays cannot be underestimated, which could further confirm the pathogenicity of the genetic variants.

KEYWORDS

EFTUD2, mandibulofacial dysostosis with microcephaly, missense mutation, prenatal diagnosis, whole-exome sequencing

This is an open access article under the terms of the [Creative Commons Attribution-NonCommercial-NoDerivs](https://creativecommons.org/licenses/by-nc-nd/4.0/) License, which permits use and distribution in any medium, provided the original work is properly cited, the use is non-commercial and no modifications or adaptations are made.

© 2022 The Authors. *Journal of Clinical Laboratory Analysis* published by Wiley Periodicals LLC.

1 | INTRODUCTION

Mandibulofacial dysostosis with microcephaly (MFDM) (MIM# 610536), also known as mandibulofacial dysostosis Guion–Almeida type, is a rare multiple malformation syndrome characterized by malar and mandibular hypoplasia, congenital- or postnatal-onset microcephaly, and dysplastic ears with associated conductive hearing loss. Intellectual disability is a prominent feature. Other major features include distinctive facial features, cleft palate, choanal atresia, and facial asymmetry. In some instances, extracranial malformations, such as esophageal atresia, congenital heart disease, and thumb abnormalities were observed. Short stature is present in approximately one-third of individuals with the condition.^{1–6}

Located on chromosome 17q21.31, the *EFTUD2* (elongation factor Tu GTP-binding domain-containing 2, OMIM: 603892) gene encodes U5-116 kD, which is a highly conserved spliceosomal GTPase and a component of the major spliceosome that processes precursor messenger RNAs (pre-mRNAs) and ligates coding sequences (exons) to form mature spliced mRNAs.^{7,8} Haploinsufficiency of *EFTUD2* has been confirmed as the main mechanism underlying MFDM.^{1–3,5,9} The majority of described *EFTUD2* mutations involved in MFDM are *de novo*, with various types of single nucleotide variants (SNVs), including frameshifts, splice sites, nonsense, and missense mutations and complete or partial gene deletions, including cytogenetically visible deletions.^{1,2,5,9–12} However, autosomal dominant inheritance from a parent with a milder phenotype, as well as germline mosaicism, has been reported.^{1,2,13}

Here, we report the case of a 16-month-old boy with MFDM and identified a novel *de novo* *EFTUD2* missense mutation (c.671G>T, p.Gly224Val) by whole-exome sequencing (WES) analysis. Additionally, we generated a zebrafish line with human *EFTUD2* disruption to investigate the function of this mutation. Therefore, we confirmed that this novel *de novo* missense mutation induced the phenotype of patients with MFDM.

2 | MATERIALS AND METHODS

2.1 | Patient

The proband was a 16-month-old boy, the first child of a healthy, non-consanguineous Chinese couple. He was delivered vaginally at 39⁺¹ weeks with a birth weight of 2760 g (–1.5 standard deviation [SD]), length of 47 cm (–2SD), and head circumference of 33 cm (–1SD). He was born with developmental disorders of the first and second branchial arches, micrognathia, a midline cleft palate, microtia, and auditory canal atresia. He was diagnosed with a Pierre-Robin sequence and admitted to the neonatal intensive care unit due to feeding difficulty. His newborn hearing screening result was abnormal. The auditory brainstem response evaluation was consistent with severe sensorineural hearing loss in both ears. The patient also presented with limited mouth opening and feeding difficulties. Computed tomography of the temporal bones showed a horizontal semicircular canal on the left side, hypoplasia, enlarged vestibular aqueduct, and malformation of the inner ear structures. His growth parameters indicated significant microcephaly (head circumference, 41 cm [–4SD]) and short stature (length, 78 cm; [–2SD]; weight, 8 kg [–3SD]). We observed that the proband had mandibular hypoplasia, malar hypoplasia, micrognathia, microtia, and auditory canal atresia. He could not sit without support and used any sign language to communicate (Figure 1). The parents of the proband came for genetic counseling while the mother was at 21 weeks of gestation. Pretest counseling was performed by trained clinical geneticists. We obtained peripheral blood samples from the proband and his parents and amniotic fluid samples from the fetus. Written informed consent was obtained from the couple before genetic testing. The study was approved by the Medical Ethics Committee of West China Second University Hospital, Sichuan University, China.



FIGURE 1 Facial photograph of the patient. Facial photograph of the patient at 16 months of age showed malar and mandibular hypoplasia, microcephaly, micrognathia, midline cleft palate, and microtia. (A) front view; (B) profile view

2.2 | Whole-exome sequencing

Genomic DNA was extracted from the peripheral blood of the proband and his parents and subjected to WES in trio. NanoWES Human Exome V1 (Berry Genomics) was used to capture the sequences. The Illumina NovaSeq6000 platform with 150-bp paired-end reads was used to sequence the enriched library. The Burrows–Wheeler Aligner software tool was used to align the sequencing reads with hg18/GRCh38. Subsequently, local alignment and recalibration of the base quality of the Burrows–Wheeler aligned reads were performed using the GATK Indel Realigner and GATK Base Recalibrator, respectively (broadinstitute.org/). GATK Unified Genotyper was used to identify SNVs and small insertions or deletions (InDels). Finally, the variants were annotated and interpreted using ANNOVAR and the Enliven Variants Annotation Interpretation System authorized by Berry Genomics.

During interpretation and analysis of the data, we filtered the variations if their minor allele frequencies were more than 0.05 in gnomAD (<http://gnomad.broadinstitute.org/>) and 1000 Genomes Project (1000G) (<http://browser.1000genomes.org/>). SNVs with minor allele frequency $\geq 1\%$ for the recessive model or $\geq 0.1\%$ for the dominant model were also excluded. The detected SNVs were systemically evaluated for pathogenicity based on the scientific and medical literature and disease databases PubMed (<https://www.ncbi.nlm.nih.gov/pubmed/>), ClinVar (<http://www.ncbi.nlm.nih.gov/clinvar/>), Human Gene Mutation Database (<http://www.hgmd.org/>), and OMIM (<http://www.omim.org/>). ACMG guidelines were used to interpret sequence variants. The detailed process for identifying the candidate variants was performed as previously described.^{14–18}

2.3 | Sanger sequencing

Sanger sequencing was performed to verify the novel mutation (c.671G>T) in exon 9 of *EFTUD2*. Primers were designed according to the *EFTUD2* sequence (GenBank NM_004247.4) as follows: forward, 5'-TCA CCA CAC CTG GCT AAT-3'; reverse, 5'-GCA AGG ATA TGA CAC TAA TGG-3'. Polymerase Chain Reaction (PCR) was performed in a total volume of 25 μ l containing 5 μ l DNA, 2.5 μ l of 10 \times buffer (MgCl₂ plus), 0.5 μ l of dNTPs, 1.5 μ l of each primer, 0.5 μ l of rTaq and 13.5 μ l of H₂O. The PCR program on a Veriti[®] 96-Well Thermal Cycler (Thermo Fisher) was performed as follows: 95°C for 10 min, followed by 35 cycles of 94°C for 40 s, 61.8°C for 30 s, and 72°C for 30 s; and 72°C for 10 min. The PCR products were sequenced using an ABI 3500 Genetic Analyzer (Thermo Fisher) for c.671G>T.

2.4 | In silico analysis and homology study

Based on the mutation (c.671G>T), possible changes in amino acids were predicted using PROVEAN (Protein Variation Effect Analyzer, version 1.1.3) and Mutation Taster (www.mutationtaster.org/,

Mutation Taster 2021), which may result from mutation identified in the proband. Homology studies have been conducted in many vertebrate species including *Rattus norvegicus*, *Mus musculus*, *Danio rerio*, *Macaca mulatta*, and *Ovis aries* (sequences obtained from www.ensembl.org).

2.5 | Prenatal diagnosis

Fetal samples were obtained through amniocentesis for single nucleotide polymorphism (SNP) array experiments at a gestational age of 21⁺⁶ weeks because of advanced maternal age. Chromosomal microarray analysis (CMA) was performed as previously described.¹⁹ Detailed second trimester fetal anomaly scans were performed by two fetal sonographers (Voluson E8; GE Medical Systems, Zipf, Austria) at a gestational age of 24⁺³ weeks. Sanger sequencing was performed to analyze the nucleotide sequence of c.671 in *EFTUD2* at a gestational age of 26⁺¹ weeks after the genetic etiology of the proband was confirmed.

2.6 | Zebrafish embryo manipulations and whole-mount *in situ* hybridization

All animals were handled in accordance with the Guide for the Care and Use of Laboratory Animals, approved by the Institutional Animal Care and Use Committee of Sichuan University, China. The human *EFTUD2* coding region sequence was synthesized by Dharmacon (catalog number OHS5893-202499238). WT zebrafish embryos from the AB strain were used in this study. Embryos were obtained by natural mating and cultured in an embryo medium.²⁰ Embryo staging was performed according to Kimmel et al.²¹ Synthetic mRNAs were then injected into single-cell embryos. The injection dose was estimated as the dose received by a single embryo. Whole-mount *in situ* hybridization was performed, as previously described by Thisse et al.²² Antisense RNA probes for *in situ* hybridization were synthesized using the DIG RNA Labeling Kit (SP6/T7) (Roche) and purified using MEGAclear (Ambion). Grayscale measurements, point mutation expression plasmid construction, and statistical analyses were performed as previously described.²³

3 | RESULTS

3.1 | A novel de novo heterozygous *EFTUD2* mutation identified in the patient with MFDM

To detect the genetic etiology of the affected individual with MFDM, trio-WES was performed on the peripheral blood samples of the family. A novel de novo heterozygous missense mutation (c.671G>T) in exon 9 of *EFTUD2* (NM_004247.4), which may lead to structural

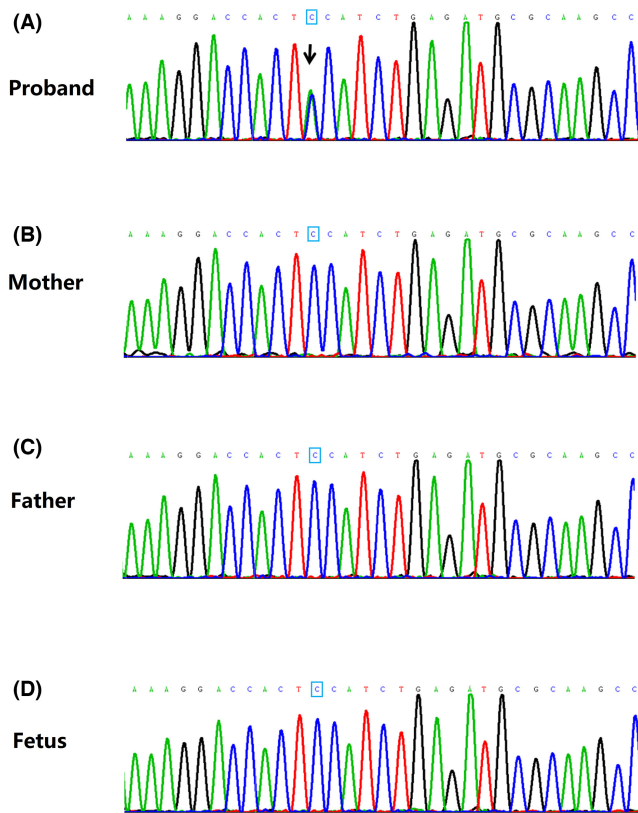


FIGURE 2 Sanger sequencing of the novel *EFTUD2* missense mutation. Whole-exome sequencing identified a novel *EFTUD2* missense mutation (c.671G>T, p.Gly224Val) in a proband with mandibulofacial dysostosis with microcephaly (MFDM). (A) Sanger sequencing confirmed the *EFTUD2* missense mutation (c.671G>T, p.Gly224Val) in blood samples from the proband; (B–D) the *EFTUD2* missense mutation (c.671G>T, p.Gly224Val) was not detected in peripheral blood samples of the proband's parents and amniotic fluid samples of the parents' second baby. Black arrows indicate the point mutation (G>T)

changes in the *EFTUD2* protein (p.Gly224Val), was identified. The presence of the mutation was confirmed by Sanger sequencing in the proband (Figure 2A) but was not detected in peripheral blood samples of the parents (Figure 2B–C).

3.2 | In silico analysis and homology study

To understand the potential impact of the c.671G>T mutation on *EFTUD2* function, in silico analysis was performed. The missense mutation (c.671G>T) resulted in a change in glycine to valine at amino acid position 224 (p.Gly224Val).

The *EFTUD2* protein (NP_004238.3), composed of 972 amino acids, contains six vital domains (the Protein Families (Pfam) database (<http://pfam.xfam.org>)): a 116 kDa U5 small nuclear ribonucleoprotein component, N-terminal (4–110 amino acids); a transcription factor, GTP-binding domain (129–377 amino acids); a translation elongation factor EFTu-like, domain 2 (491–566 amino acids); an elongation factor G, domain III (586–648 amino acids); a translation

elongation factor EFG/EF2, domain IV (707–823 amino acids); and an elongation factor EFG, domain V-like (826–914 amino acids).

Amino acid 224 was located within the transcription factor, GTP-binding domain, and prior to the translation elongation factor EFTu-like domain 2 (Figure 3). PROVEAN and MutationTaster were used to predict the pathogenicity of the mutation (p.Gly224Val) in *EFTUD2*, which revealed that the mutation was deleterious. Gly224 is highly conserved among various vertebrate species (Figure 4), suggesting that it plays an important role in *EFTUD2* function.

3.3 | Prenatal diagnosis for the fetus

Chromosomal aberrations of the fetus were excluded using SNP array analysis. According to the ACMG 2015 guidelines,²⁴ the c.671G>T mutation is classified as likely pathogenic (PS2, PM1, PM2, and PP3). Sanger sequencing of amniotic fluid samples was performed, and the mutation c.671 of *EFTUD2* was excluded (Figure 2D). Ultrasound abnormalities, including microcephaly, micrognathia, microtia, cleft palate, and heart defects, were excluded. The fetus was delivered vaginally at 39⁺⁶ weeks of age with a birth weight of 3150 g, length of 49 cm, and head circumference of 33.5 cm. After 14 months of clinical follow-up by the pediatricians, no abnormal phenotypes were detected.

3.4 | p.Gly224Val mutation found in human leads to loss of function of *EFTUD2* in zebrafish model

To determine whether the *EFTUD2* c.671G>T mutation led to loss of function in vivo, we synthesized mRNAs of human *EFTUD2* and its mutation and injected them into zebrafish embryos.

Based on clinical symptoms, we investigated brain and heart development during embryogenesis by marker analyses using whole-mount *in situ* hybridization. Results showed that expression of the hindbrain neuron marker *pax2a* decreased significantly in ~30 pg *EFTUD2* WT mRNA-injected embryos with a percentage of 32% at indicated stages; heart development marked by cardiac marker *myl7* showed that *EFTUD2* WT mRNAs induced looping defects in 22% of embryos, and 23% of small head phenotype was also observed in embryos injected with *EFTUD2* WT mRNAs. Embryos injected with the same doses of *EFTUD2* p.Gly224Val mutant mRNAs showed a decreased percentage of abnormal effects on brain and heart development.

Furthermore, only 12% of the embryos showed decreased *pax2a* expression, 11% of the embryos showed looping defects stained by *myl7*, and 15% of the embryos showed small heads detected by *sox3* (Figure 5). Taken together, these results demonstrate that the *EFTUD2* c.671G>T mutation causes loss of gene function in *EFTUD2*.

4 | DISCUSSION

Mandibulofacial dysostosis with microcephaly is a rare autosomal dominant disease characterized by malar and mandibular hypoplasia,

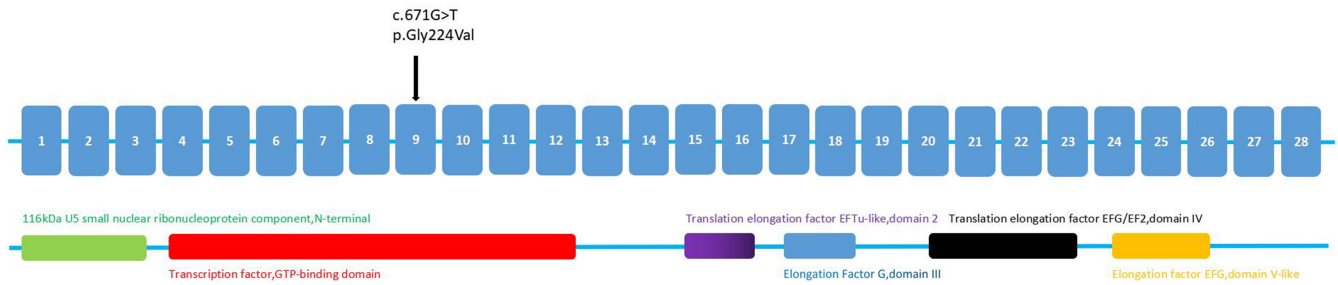
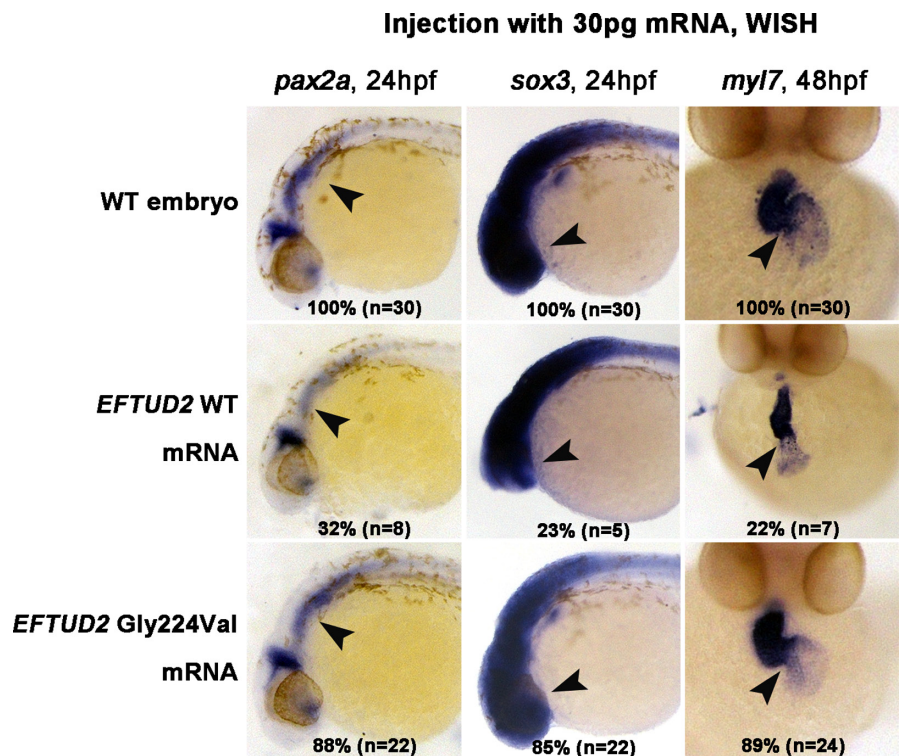


FIGURE 3 Protein domains and location of mutation in *EFTUD2*. The missense mutation (c.671G>T) in *EFTUD2* was located within the transcription factor GTP-binding domain, and prior to translation elongation factor EFTu-like, domain 2. Black arrows indicate the point mutation (G>T)

FIGURE 4 Gly224 is highly conserved in many vertebrate species

	224																							
<i>Homo sapiens</i> (human)	D	E	V	T	A	G	L	R	I	S	D	G	V	V	L	F	I	D	A	A	E	G		
<i>Rattus norvegicus</i> (Norway rat)	D	E	V	T	A	G	L	R	I	S	D	G	V	V	L	F	I	D	A	A	E	G		
<i>Mus musculus</i> (house mouse)	D	E	V	T	A	G	L	R	I	S	D	G	V	V	L	F	I	D	A	A	E	G		
<i>Danio rerio</i> (zebrafish)	D	E	V	T	S	A	V	R	L	S	D	G	V	V	L	F	I	D	A	A	E	G		
<i>Macaca mulatta</i> (Rhesus monkey)	D	E	V	T	A	G	L	R	I	S	D	G	V	V	L	F	I	D	A	A	E	G		
<i>Ovis aries</i> (sheep)	D	E	V	T	A	G	L	R	I	S	D	G	V	V	L	F	I	D	A	A	E	G		

FIGURE 5 p.Gly224Val mutation leads to loss of function of *EFTUD2* in the zebrafish model. p.Gly224Val mutation caused a loss of gene function of *EFTUD2* during zebrafish embryogenesis. The *EFTUD2* p.Gly224Val mutant mRNA decreased percentage of abnormality of embryonic neurodevelopment and cardiac development compared to *EFTUD2* WT mRNA. Expression of *pax2a* and *sox3* at 24 hpf, *myl7* at 48 hpf, embryos at 24 hpf shown are lateral views with anterior to the left, embryos at 48 hpf shown are ventral view with the anterior at the top. Arrows point to the signal generated by detected marker genes. The percentage and numbers indicated in each image are the ratio for the number of affected embryos with phenotype similar to what is shown in the picture



microcephaly, external ear abnormalities, hearing loss, and intellectual disability.⁹ The prevalence of MFDM has been reported to be <1 in 1,000,000 individuals.²⁵ In this study, we report the case of a 16-month-old boy with MFDM and identified a novel *de novo* *EFTUD2* missense mutation (c.671G>T, p.Gly224Val) by trio-WES analysis.

Traditionally, disease diagnosis has been phenotype-driven. The phenotypes overlap among craniofacial disorders, such as oculo-auriculo-vertebral spectrum, CHARGE syndrome, Pierre-Robin

sequence, and Treacher-Collins syndrome, which presents a major challenge in confirming a definitive diagnosis.²⁶⁻²⁹ The proband in our study was initially diagnosed with a Pierre-Robin sequence because of micrognathia, cleft palate, and feeding difficulty. However, the increased application of next-generation sequencing has successfully identified thousands of causative pathogenic variants for rare disorders, especially in unrelated sporadic cases or in affected families with small pedigrees. In our study, trio-WES revealed a novel heterozygous mutation in *EFTUD2* of the proband and confirmed the

clinical diagnosis of MFDM. Furthermore, prenatal examination for the mutation was performed to ensure the birth of an unaffected fetus.

EFTUD2, a core spliceosome U5 small nuclear ribonucleoprotein gene, encodes a component of the major spliceosome and causes MFDM because of the heterozygous loss-of-function (LoF) mutations.⁹ The *de novo* *EFTUD2* missense mutation (c.671G>T, p.Gly224Val) identified in our study has not previously been reported in the literature and is absent from the PubMed and Disease databases (GnomAD, 1000 Genomes, OMIM, PubMed, ClinVar, and HGMD). Meanwhile, amino acid 224 was located within the GTP-binding domain of the transcription factor. *In silico* analysis predicted that this mutation was deleterious. Thus, the c.671G>T mutation was classified as likely to be pathogenic.

Gordon et al.³⁰ reported the case of a patient with malar and mandibular hypoplasia, bilateral microtia, sensorineural hearing loss, moderate intellectual disability, and epilepsy. Sequencing of *EFTUD2* revealed a heterozygous missense mutation (c.670G>A) that led to a change in glycine to arginine at amino acid position 224 (p.Gly224Arg), which is similar to the change in amino acid residue in our study (c.671G>T, p.Gly224Val). However, prediction of the potential pathogenic effect of the missense mutation has been based solely on *in silico* analysis, which lacks functional experimental studies. Furthermore, Thomas et al.³¹ performed functional assays in yeast *SNU114* to investigate the effect of *EFTUD2* missense variants on *EFTUD2* protein function. However, it is still unclear how the *EFTUD2* missense variants (c.671G>T, p.Gly224Val) cause inactivation of an allele and haploinsufficiency.

In our study, the pathogenic effects of the variant were demonstrated using rigorous functional analysis of a zebrafish line with human *EFTUD2* disruption. The abnormal effect on brain and heart development in embryos injected with *EFTUD2* p.Gly224Val mutant mRNAs was decreased compared with *EFTUD2* WT mRNAs injected embryos, which demonstrated that the *EFTUD2* c.671G>T mutation caused a loss of gene function in *EFTUD2*. Thus, the *EFTUD2* c.671G>T mutation was classified as pathogenic (PS2, PS3, PM1, and PM2).

In conclusion, while WES is a useful tool for identifying potentially pathogenic mutations, especially in rare disorders, the importance of functional assays cannot be underestimated. We first identified a novel *EFTUD2* c.671G>T mutation in a Chinese patient with MFDM and confirmed the pathogenicity of the mutation (p.Gly224Val) by functional assay in zebrafish. Based on our findings, prenatal diagnosis was performed on the second baby of the proband's parents to exclude the *EFTUD2* mutation, and it was confirmed that the baby did not have the MFDM phenotype after 14 months of follow-up.

ACKNOWLEDGMENT

This work was supported by National Key Research and Development Program of China (2021YFC1005304).

CONFLICT OF INTEREST

None.

AUTHOR CONTRIBUTIONS

MY, HQS, and TH designed the study. YYL and ZYL performed the experiments. MY, YYL, HQS, and TH conducted data analysis. All authors read and approved the final manuscript.

ETHICS APPROVAL AND CONSENT TO PARTICIPATE

The present study was approved by the Medical Ethics Committee of West China Second University Hospital of Sichuan University. Written informed consent to participate was obtained from the parents of the patient.

PATIENT CONSENT FOR PUBLICATION

Written informed consent for publication was obtained from the parents of the patient.

DATA AVAILABILITY STATEMENT

All data generated or analyzed during this study are included in this published article.

ORCID

Mei Yang  <https://orcid.org/0000-0002-6200-5865>

Yanyan Liu  <https://orcid.org/0000-0003-0894-9344>

Huaqin Sun  <https://orcid.org/0000-0002-4548-4657>

Ting Hu  <https://orcid.org/0000-0002-4642-3848>

REFERENCES

- Huang L, Vanstone MR, Hartley T, et al. Mandibulofacial dysostosis with microcephaly: mutation and database update. *Hum Mutat.* 2016;37(2):148-154.
- Lines M, Hartley T, MacDonald SK, Boycott KM. *Mandibulofacial Dysostosis with Microcephaly*. *GeneReviews*[®] [Internet]. University of Washington, Seattle; 1993-2020.
- Luquetti DV, Hing AV, Rieder MJ, et al. "Mandibulofacial dysostosis with microcephaly" caused by *EFTUD2* mutations: expanding the phenotype. *Am J Med Genet A.* 2013;161A(1):108-113.
- Wieczorek D, Shaw-Smith C, Kohlhase J, et al. Esophageal atresia, hypoplasia of zygomatic complex, microcephaly, cup-shaped ears, congenital heart defect, and mental retardation—new MCA/MR syndrome in two affected sibs and a mildly affected mother? *Am J Med Genet A.* 2007;143A(11):1135-1142.
- Lines MA, Huang L, Schwartzenuber J, et al. Haploinsufficiency of a spliceosomal GTPase encoded by *EFTUD2* causes mandibulofacial dysostosis with microcephaly. *Am J Hum Genet.* 2012;90(2):369-377.
- Guion-Almeida ML, Zechi-Ceide RM, Vendramini S, Tabith JA. A new syndrome with growth and mental retardation, mandibulofacial dysostosis, microcephaly, and cleft palate. *Clin Dysmorphol.* 2006;15(3):171-174.
- Fabrizio P, Lagerbauer B, Lauber J, Lane WS, Lüthmann R. An evolutionarily conserved U5 snRNP-specific protein is a GTP-binding factor closely related to the ribosomal translocase EF-2. *EMBO J.* 1997;16(13):4092-4106.
- Johnson TL, Vilardell J. Regulated pre-mRNA splicing: The ghostwriter of the eukaryotic genome. *Biochim Biophys Acta.* 2012;1819(6):538-545.
- Lehalle D, Gordon CT, Oufadem M, et al. Delineation of *EFTUD2* haploinsufficiency-related phenotypes through a series of 36 patients. *Hum Mutat.* 2014;35(4):478-485.
- Rengasamy Venugopalan S, Farrow EG, Lypka M. Whole-exome sequencing identified a variant in *EFTUD2* gene in establishing a genetic diagnosis. *Orthod Craniofac Res.* 2017;20(Suppl 1):50-56.

11. Kim SY, Lee DH, Han JH, Choi BY. Novel splice site pathogenic variant of EFTUD2 is associated with mandibulofacial dysostosis with microcephaly and extracranial symptoms in Korea. *Diagnostics (Basel)*. 2020;10(5):296.
12. Sarkar A, Emrick LT, Smith EM, et al. Novel de novo mutations in EFTUD2 detected by exome sequencing in mandibulofacial dysostosis with Microcephaly syndrome. *Am J Med Genet A*. 2015;167A(4):914-918.
13. Lacour JC, McBride L, St Hilaire H, et al. Novel de novo EFTUD2 mutations in 2 cases with MFD, initially suspected to have alternative craniofacial diagnoses. *Cleft Palate Craniofac J*. 2019;56(5):674-678.
14. Yang M, Xu B, Wang J, et al. Genetic diagnoses in pediatric patients with epilepsy and comorbid intellectual disability. *Epilepsy Res*. 2021;170:106552. doi:[10.1016/j.eplepsyres.2021.106552](https://doi.org/10.1016/j.eplepsyres.2021.106552)
15. Han P, Wei G, Cai K, et al. Identification and functional characterization of mutations in LPL gene causing severe hypertriglyceridaemia and acute pancreatitis. *J Cell Mol Med*. 2020;24(2):1286-1299.
16. Zhang R, Chen S, Han P, et al. Whole exome sequencing identified a homozygous novel variant in CEP290 gene causes Meckel syndrome. *J Cell Mol Med*. 2020;24(2):1906-1916.
17. Dai Y, Liang S, Dong X, et al. Whole exome sequencing identified a novel DAG1 mutation in a patient with rare, mild and late age of onset muscular dystrophy-dystroglycanopathy. *J Cell Mol Med*. 2019;23(2):811-818.
18. Zheng Y, Xu J, Liang S, et al. Whole exome sequencing identified a novel heterozygous mutation in HMBS gene in a Chinese patient with acute intermittent porphyria with rare type of mild anemia. *Front Genet*. 2018;9:129.
19. Hu T, Tian T, Zhang Z, et al. Prenatal chromosomal microarray analysis in 2466 fetuses with ultrasonographic soft markers: A prospective cohort study. *Am J Obstet Gynecol*. 2020;S0002-9378(20):31269-31272.
20. Westerfield M. *The Zebrafish Book*. University of Oregon Press; 1993.
21. Kimmel CB, Ballard WW, Kimmel SR, et al. Stages of embryonic development of the zebrafish. *Dev Dyn*. 1995;203(3):253-310.
22. Thisse C, Thisse B. High-resolution in situ hybridization to whole-mount zebrafish embryos. *Nat Protoc*. 2008;3(1):59-69.
23. Sun H, Wang Y, Zhang J, et al. CFTR mutation enhances Dishevelled degradation and results in impairment of Wnt-dependent hematopoiesis. *Cell Death Dis*. 2018;9(3):275.
24. Richards S, Aziz N, Bale S, et al. ACMG laboratory quality assurance committee. standards and guidelines for the interpretation of sequence variants: a joint consensus recommendation of the American college of medical genetics and genomics and the association for molecular pathology. *Genet Med*. 2015;17(5):405-424.
25. Silva JB, Soares D, Leão M, Santos H. Mandibulofacial dysostosis with microcephaly: a syndrome to remember. *BMJ Case Rep*. 2019;12(8):e229831.
26. Beleza-Meireles A, Clayton-Smith J, Saraiva JM, Tassabehji M. Oculo-auriculo-vertebral spectrum: A review of the literature and genetic update. *J Med Genet*. 2014;51(10):635-645.
27. van Ravenswaaij-Arts C, Martin DM. New insights and advances in CHARGE syndrome: Diagnosis, etiologies, treatments, and research discoveries. *Am J Med Genet C Semin Med Genet*. 2017;175(4):397-406.
28. Cladis F, Kumar A, Grunwaldt L, Otteson T, Ford M, Losee JE. Pierre Robin Sequence: A perioperative review. *Anesth Analg*. 2014;119(2):400-412.
29. Wiczorek D, Gener B, González MJ, et al. Microcephaly, microtia, preauricular tags, choanal atresia and developmental delay in three unrelated patients: a mandibulofacial dysostosis distinct from Treacher Collins syndrome. *Am J Med Genet A*. 2009;149A(5):837-843.
30. Gordon CT, Petit F, Oufadem M, et al. EFTUD2 haploinsufficiency leads to syndromic oesophageal atresia. *J Med Genet*. 2012;49(12):737-746.
31. Thomas HB, Wood KA, Buczek WA, et al. EFTUD2 missense variants disrupt protein function and splicing in mandibulofacial dysostosis Guion-Almeida type. *Hum Mutat*. 2020;41(8):1372-1382.

How to cite this article: Yang M, Liu Y, Lin Z, Sun H, Hu T. A novel de novo missense mutation in EFTUD2 identified by whole-exome sequencing in mandibulofacial dysostosis with microcephaly. *J Clin Lab Anal*. 2022;36:e24440. doi:[10.1002/jcla.24440](https://doi.org/10.1002/jcla.24440)